Earth Surf. Dynam. Discuss., doi:10.5194/esurf-2017-8, 2017
Manuscript under review for journal Earth Surf. Dynam.
Discussion started: 1 March 2017

Multiple controls on sediment grain properties of Peruvian coastal river basins

Camille Litty[1], Fritz Schlunegger[1], Willem Viveen[2]

[1] Institute of Geological Sciences, University of Bern, Baltzerstrasse 1+3, CH- 3012 Bern.

[2] Sección de Ingeniería de Minas e Ingeniería Geológica, Departamento de Ciencias e Ingeniería, Pontificia Universidad Católica del Perú, San Miguel, Lima, Perú.

ABSTRACT

Twenty-one coastal rivers located on the western Peruvian margin were analyzed to determine the relationships between fluvial and environmental processes and sediment grain properties such as grain size, roundness and sphericity. Modern gravel beds were sampled along a north-south transect on the western side of the Peruvian Andes, and at each site the long *a*-axis and the intermediate *b*-axis of about 500 pebbles were measured. Morphometric properties such as river gradient, catchment size and discharge of each drainage basin were determined and compared against measured grain properties. Grain size data show a constant value of the D_{50} percentile all along the coast, but an increase in the D_{84} and D_{96} values and an increase in the ratio of the intermediate and the long axis from south to north. Our results then yield better-sorted and less spherical material in the south when compared to the north. No correlations were found between the grain size and the morphometric properties of the river basins when considering the data together. Grouping the results in a northern and southern group shows better-sorted sediments and lower D_{84} and D_{96} values for the southern group of basins. Within

Earth Surf. Dynam. Discuss., doi:10.5194/esurf-2017-8, 2017
Manuscript under review for journal Earth Surf. Dynam.
Discussion started: 1 March 2017

the two groups, correlations were found between the grain size distributions and morphometric basins properties. Our data indicates that fluvial transport is the dominant process controlling the erosion, transport and deposition of sediment in the southern basins while we propose a geomorphic control on the grain size properties in the northern basins. Sediment properties in the northern and southern basins could not be linked to differences in tectonic controls. On the other hand, the north-south trend in the grain size and in the b/a ratio seems controlled by a shift towards a more humid climate and towards a stronger El Nino impact in northern Peru. But, generally speaking, the resulting trends and differences in sediment properties seem controlled by differences in the complex geomorphic setting along the arc and forearc regions.

1. INTRODUCTION

The size and shape of gravel bears crucial information about the transport dynamics of mountain rivers (Hjulström, 1935; Shields, 1936; Blissenbach, 1952; Koiter et al., 2013; Whittaker et al., 2007; Duller et al., 2012; Attal et al., 2015), about sediment provenance (Parker, 1991; Paola et al., 1992a, b; Attal and Lavé, 2006) and about environmental conditions such as uplift and precipitation (Heller and Paola, 1992; Robinson and Slingerland, 1998; Foreman et al., 2012; Allen et al., 2013; Foreman, 2014). The mechanisms by which grain size and shape change from source to sink have often been studied with flume experiments (e.g. McLaren and Bowles, 1985; Lisle et al., 1993) and numerical models (Hoey, 2010). These studies have mainly been directed towards exploring the controls on the downstream reduction in grain size of gravel beds (Schumm and Stevens, 1973; Hoey and Fergusson, 1994; Surian, 2002; Fedele and Paola, 2007). Less attention has, however, been paid to external controls such as climate and tectonic change as well as a complex geomorphic setting on grain size properties.

Earth Surf. Dynam. Discuss., doi:10.5194/esurf-2017-8, 2017
Manuscript under review for journal Earth Surf. Dynam.
Discussion started: 1 March 2017

Here, we present data on sediment grain properties from streams situated on the western margin of the Peruvian Andes (Figure 1A) in order to elucidate the effects of precipitation, hydrological properties, catchment morphometrics, tectonics and the El Niño on those sedimentological characteristics. We will show that differences in tectonic regime do not influence sediment properties, whereas climate anomalies such as the El Niño effect, internal river dynamics, supply patterns and geomorphic setting seem to be the most important factors for determining sediment size and shape.

1.1 Geologic and tectonic setting

The study area is located at the transition from the Peruvian Andes to the coastal lowlands along a transect from the cities of Trujillo in the north (8°S) to Tacna in the south (18°S). In northern and central Peru, a flat, up-to 100 km, broad coastal forearc plain with Paleogene-Neogene and Quaternary sediments (Gilboa, 1977) connects to the western Cordillera. This part of the western Cordillera consists of Cretaceous to late Miocene plutons of various compositions (diorite, but also tonalite, granite and granodiorite) that crop out over an almost continuous 1600-km long arc that is referred to as the Coastal Batholith (e.g. Atherton, 1984; Mukasa, 1986; Haederle and Atherton, 2002; Figure 1B). In southern Peru, the coastal plain gives way to the Coastal Cordillera that extends far into Chile. The western Cordillera comprises the central volcanic arc region of the Peruvian Andes with altitudes of up to 6768 m.asl, where currently active volcanoes south of 14°S of latitude are related to a steep slab subduction. Contrariwise, Cenozoic volcanoes in the central and northern Peruvian arc have been extinct since c. 11 Ma due to a flat slab subduction, which inhibited magma upwelling from the asthenosphere (Ramos, 2010).

Earth Surf. Dynam. Discuss., doi:10.5194/esurf-2017-8, 2017
Manuscript under review for journal Earth Surf. Dynam.
Discussion started: 1 March 2017

The bedrock of the Western Cordillera is dominated by Paleogene, Neogene and Quaternary volcanic rocks (mainly andesitic or dacitic tuffs, and ignimbrites) originating from distinct phases of Cenozoic volcanic activity (Vidal, 1993). These rocks rest on Mesozoic and Early Tertiary sedimentary rocks (Figure 1B). In southern Peru, the segment with steep subduction hosts raised Quaternary marine terraces (Saillard et al., 2011) (Figure 1A). This suggests the occurrence of surface uplift south of 15°S of latitude, while the region dominated by flat slab subduction has most likely subsided at least during the Quaternary (Macharé et al., 1986). Because of these inferences, we expect to see a tectonic control on grain size distribution through larger clasts south of 15°S of latitude compared to the segment north of it.

The local relief along the western Cordillera has been formed by deeply incising rivers that flow perpendicular to the strike of the Andes (Schildgen et al., 2007; 2009). The morphology of the longitudinal stream profiles is characterized by two segments separated by a distinct knickzone (Figure 2; Trauerstein et al., 2013). These geomorphic features have formed through headward retreat in response to a phase of enhanced surface uplift during the late Miocene (e.g., Schildgen et al., 2007). Upstream of these knickzones, the streams are mainly underlain by Tertiary volcanoclastic rocks, while farther downstream incision has disclosed the Coastal Batholith and older meta-sedimentary units (Trauerstein et al. 2013). The upstream edges of these knickzones also delineate the upper boundaries of the major sediment sources (Litty et al., 2017). Contrariwise, little to nearly zero clastic material has been derived from the headwater reaches in the Altiplano, where the flat landscape has experienced nearly zero erosion, as 10Be-based denudation rate estimates (Abbühl et al., 2011) and provenance tracing have shown (Litty et al., 2017).

Earth Surf. Dynam. Discuss., doi:10.5194/esurf-2017-8, 2017
Manuscript under review for journal Earth Surf. Dynam.
Discussion started: 1 March 2017

1.2 Climatic setting

The N-S-oriented, annual rainfall rates decrease from 1000 mm per year near the Equator to 0 mm along the coast in southern Peru and northern Chile (Huffman et al., 2007; Figure 1C). The Peruvian western margin shows an E-W contrasting precipitation pattern with high annual precipitation rates up to 800 mm on the Altiplano and c. 0 mm per year on the coast (Figure 1C). This precipitation gradient in the western Andes is related to the position of the Intertropical Convergence Zone (ITCZ, inset of Figure 1C) associated with an orographic effect on the eastern side of the Andes (Bookhagen and Strecker, 2008). During austral summer (January) the center of the ITCZ is located farther south, transferring the moisture from the Amazon tropical basin to the Altiplano (Garreaud et al., 2009) and leading to a wet climate on the Altiplano with strong precipitation rates. During austral winter, the Altiplano is under the influence of dry air masses from the subsiding branch of the Hadley cell that result in a more equatorial position of the ITCZ and in a dry persistent westerly wind with almost no precipitation on the Altiplano. Additionally, the dry coast is due to the Humboldt Current, which advects cold waters from the Antarctica, cooling down the ocean along the coast. This causes an inverse climate gradient in which hot air cannot sufficiently rise and is trapped against the Andean foothills. The hot air then cools down at high altitudes in the atmosphere thereby inhibiting precipitation. Additionally, the Andes form an orogenic barrier preventing Atlantic winds and rain to reach the coast. Only around Piura, situated in northern Peru at 5°S latitude, the ocean water sufficiently warms up because of the mixing with the tropical current derived from Ecuador, resulting in precipitation in northern Peru. In addition, every 2 to 10 years, near to the Equator, the Pacific coast is subjected to strong precipitation resulting in high flood variability, related to El Nino weather phenomenon (ENSO) (DeVries, 1987).

Earth Surf. Dynam. Discuss., doi:10.5194/esurf-2017-8, 2017
Manuscript under review for journal Earth Surf. Dynam.
Discussion started: 1 March 2017

2. SITE SELECTION AND METHODS

The selected rivers are located along a transect from Trujillo in the north (8°S) to Tacna (18°S) in the south parallel to the Pacific side of the Peruvian Andes (Figure 1A). From north to south, climate becomes generally drier along the coast, with the northern area being susceptible to changes in climate due to the El Niño phenomenon. Also, the tectonic regime changes from little tectonic uplift of the forearc, north of Pisco, to rapid uplift south of Pisco. The grain size data from the selected rivers will therefore be used to identify possible trends (or lacks thereof) along strike of the Peruvian Andes. Additionally, the Majes catchment (marked with red color on Figure 1A), which is part of the 21 studied basins, has been sampled at five sites from upstream to downstream to explore the effects related to the sediment transport processes for a section across the mountain belt, but along stream (Figure 2). The Majes basin has been chosen because of its easy accessibility in the upstream direction. For the other basins, sampling sites were mostly accessible along the Pan-American Highway (see Table 1 for the coordinates of the sampling sites).

At each site, around ten digital images were taken for grain size analysis with the software program Image J (Rasband, 1997). It has been shown that using a standard frame with fixed dimensions to assist gravel sampling reduces user-biased selection of gravels (Marcus et al., 1995; Bunte and Abt, 2001a). In order to reduce this bias, we substituted the frame by shooting an equal number of photos at a fixed distance from the ground surface. Photos were taken from an approximately $10m^2$-large area to take potential spatial variabilities among the gravel bars into account. From those photos, the intermediate *b*-axes of around 500 pebbles were

Earth Surf. Dynam. Discuss., doi:10.5194/esurf-2017-8, 2017
Manuscript under review for journal Earth Surf. Dynam.
Discussion started: 1 March 2017

measured, and 500 additional pebbles were used to estimate the ratio between the *b*-axes and long *a*-axes (Bunte and Abt, 2001b). Our sample population exceeds the minimum number of samples needed for statistically reliable estimations of grain size distributions in gravel bars (Howard, 1993; Rice and Church, 1998). The pebbles were characterized on the basis of their median (D_{50}), the coarse (D_{84}) and the maximum (D_{96}) fractions. This means that 50%, 84% and 96% of the sampled fraction is finer than the 50^{th}, 84^{th} and 96^{th} percentile of the samples. On a gravel bar, pebbles tend to lie with their short axis perpendicular to the surface, thus exposing their section that contains the *a*- and *b*-axes (Bunte and Abt, 2001b). However, the principal limitation is the inability to accurately measure the fine particles < 3 mm (see also Whittaker et al., 2010). While we cannot resolve this problem with the techniques available, we do not expect that this adds a substantial bias in the grain size distributions reported here as their relative contributions to the point-count results are minor (i.e. < 5%, based on visual inspection of the digital images).

Grain size distributions of modern bars were then compared to stream runoff, river and basin morphometric properties. River discharge estimates were extracted from the results of annual surveys performed by the National Water Agency of Peru (Autoridad Nacional del Agua, 2016; Table 1). The averaged river gradients and widths at the sampling sites were extracted over a 500-m-long river profile from satellite images and orthophotos. The upstream contributing area of the basins was extracted from the 90-m digital elevation model Shuttle Radar Topography Mission (SRTM) ~90-m resolution (NASA; Table 1).

3. RESULTS

3.1 North-south pattern of grain sizes

Earth Surf. Dynam. Discuss., doi:10.5194/esurf-2017-8, 2017
Manuscript under review for journal Earth Surf. Dynam.
Discussion started: 1 March 2017

Earth Surface Dynamics
Open Access
Discussions

The results of the grain size measurement reveal a large variation for the *b*-axis where the values of the D_{50} range from 1.3 cm to 5.5 cm from northern to southern Peru (Figure 3A; Table 1). Likewise, values for the D_{84} vary between 3 cm and 10.5 cm with an increase of the values in the order of c. 0.05 mm/km from south to north (Figure 3A). The sizes for the D_{96} reveal the largest spread, ranging from 6 cm to 31 cm with a generally larger increase (0.15 mm/km towards the north) compared to the D_{50} and D_{84} values. The difference between the D_{50} and the D_{96} is smaller in the south than in the north indicating that sediments are better sorted in the south (Figure 3A). In addition, the ratios between the *b*-axis and *a*-axis (sphericity ratio) increase from south to north indicating that the pebbles are more spherical in the north (Figure 3B).

Another way to analyze the results is to separate the data in two basin groups. The motivation for this grouping lies in the differences in the tectonic conditions with normal slab subduction and an uplifting coast south of 15°S, and flat slab subduction and a flat coastal topography north of 15°S latitude (see above). We thus expect to unravel possible differences in grain size properties in response to these different morphotectonic conditions. Note that in the streams located between 15.6°S and 13.7°S, no gravel bars are encountered along the coast and only sand bars can be found, and therefore no results are exhibited (Figure 3A and B).

3.2 The Majes basin

The D_{50} percentile of the *b*-axis decreases from 6.2 cm at 106 km river upstream to a value of 5.2 cm at 20 km upstream for the Pacific coast (Figures 2 and 4 and Table 2). Likewise, the D_{84} decreases from 19 cm to 8.7 cm, and the D_{96} decreases from 31 cm to 11.6 cm (Figure 4). Geomorphologists widely accept the notion that downstream hydraulic geometry of alluvial channels reflects the decrease of particle size within an equilibrated system involving flow,

Earth Surf. Dynam. Discuss., doi:10.5194/esurf-2017-8, 2017
Manuscript under review for journal Earth Surf. Dynam.
Discussion started: 1 March 2017

channel gradient, sediment supply and transport. Sternberg (1875) formalized these relations and predicted an exponential decline in particle size in gravel bed rivers as a consequence of abrasion as the gravel is transported downstream. The relation follows the form: $D_x = D_0\, e^{-\alpha x}$ (Sternberg, 1875). Here, the exponent α decreases from 0.3 for the largest percentile (i.e., the D_{96}) to c. 0.1 for the D_{50}.

3.3 Correlations between grain sizes and morphometric properties

If all river basins are considered, without grouping them into northern and southern domains, no distinct positive nor negative correlations were found between the D_{50}, D_{84} and D_{96} percentiles of the gravel size and the long-stream distance to the knickzone reaches where the main sediment sources are located (Figure 5A and B). Likewise, no correlations have been identified between the grain size and the local river gradient (Figure 5C and 5D). Also no correlations have been found between the different grain size percentiles and the annual mean (Figure 5E) and maximum water discharge estimates (Figure 5F).

Contrariwise, positive correlations do exist between the grain size distributions and the river properties when the results are separated into northern and southern domains (see Figure 1). In the southern group of basins, a positive, yet weak, correlation has been found between the D_{50} and the mean runoff if normalized over the catchment area (Figure 6A; Table 1). The normalization has been made to identify the controls of effective precipitation on the grain size distribution. In particular, this normalization allows to identify the amount of rainfall per year, which explicitly contributes to runoff (after absorption of water through groundwater and evapotranspiration). Contrariwise, in the northern basins, a positive correlation has been found between the river gradient at sampling site and the D_{96} (Figure 6B).

4. DISCUSSION

4.1 Downstream fining trends at Majes indicates fluvial controls

In fluvial environments the sorting of the sediment depends on the downstream distance from its source (Hoey and Ferguson, 1994; Kodoma, 1994; Paola and Seal, 1995). This is particularly the case for the Majes river, where the sorting gets better in the downstream direction. In particular, we do see an exponential downstream fining trend of the three percentiles in the Majes river (Figure 4). This is somewhat surprising because sufficiently voluminous sediment input from other sources may perturb any downstream fining trends in the grain size distribution (Rice and Church, 1998). Likewise, in the Majes basin, the sediment supply from the hillslopes to the trunk stream has occurred mainly through debris flow processes and landsliding (Steffen et al., 2010; Margirier et al., 2015). Therefore, the exponential downstream fining indicates that in the Majes basin fluvial transport is the dominating process controlling the transport and evacuation of sediment from their sources down to the Pacific Ocean.

4.2 Lack of tectonic controls suggests a geomorphic influence on grain size patterns

No correlations were found between the presence or absence of the uplifted coast and the grain size distributions. Indeed, we would expect larger grain sizes where the area is uplifting through an increase of the river gradient, unless the rivers are able to compensate any uplift by incision in the underlying bedrock or alluvium. In that case the rivers remain in a state of semi-equilibrium without a change in river gradient, particularly along their lower flat segments (Bull, 1991; Maddy, 1997; Viveen et al., 2013). The fact that this is not the case here is demonstrated by the steep river profiles and pronounced knickzones (Schildgen et al., 2009). Interestingly, we see the contrary in our data: smaller and better sorted grains in the uplifted coastal area where the drainage basins are larger, and larger grains with a lower degree of sorting in the north where recent uplift seems to be lacking and where the sizes of the catchments are relatively small. We thus infer primarily a geomorphic control based on these relationships where smaller rivers in smaller basins are less capable of sorting the material upon transport.

4.3. Climatic control

In addition to the geomorphic control on grain size inferred here through correlations between basin morphometric properties and grain size distributions, a general south-north increasing trend in grain size is visible that overlies the patterns discussed earlier (Figure 3). Large-magnitude, low-frecuency rainfall events are an important driver for catchment-scale soil erosion over variable temporal scales (Baartman et al., 2013). Floods in temperate environments are generally characterized by larger magnitudes when compared to arid regions if similar upstream basin sizes are considered (Molnar et al., 2006). This could provide an explanation for the generally larger grain sizes in the north compared to the south, certainly if they are associated with periodic glacial melt. In particular, a more humid climate, as is the case in northern Peru, could induce larger floods (compared to the south) with the effect that the material will be transported more efficiently compared to the southern domains. We acknowledge, however, that a lack of vegetation in arid climates such as in the south can lead to more intensely erosion (Morgan and Rickson, 2003). We also note that the coastal area of northern Peru is subjected to El Niño precipitation events yielding larger flood variability (Wells, 1990; Garreaud and Aceituno, 2001), which could also explain why the river sediments tend to be larger and worse sorted.

Earth Surf. Dynam. Discuss., doi:10.5194/esurf-2017-8, 2017
Manuscript under review for journal Earth Surf. Dynam.
Discussion started: 1 March 2017

4.4 Possible controls of a complex pattern of sediment supply

In addition to the aforementioned controls, it is possible that the generally S-N increasing trend in grain size reflects, at a smaller scale, the complexity of processes and hillslope-channel coupling relationships, paired with contrasts in fractures of bedrock and effects related to glacial pre-conditioning. This complexity of morphology and bedrock lithologies complicates the interpretation of grain size patterns. As an example, the uplifted, flat Moquegua graben system (c. 17°S; Decou et al., 2011) forms the headwaters of the southern rivers, and those rivers are also famous for their agricultural terraces (pre)dating Inca times (e.g. Londoño, 2008). Alluvial fans are also very common in those basins (Steffen et al., 2010). Such flat, stepped elements generally decrease the amount of landscape erosion (Baartman et al., 2013) and halt the incorporation of larger, primarily gravity-driven rocks and boulders into the fluvial system. Contrariwise, the headwaters of the northern basin group encompass the largest area of tropical glaciers in the world (Rabatel et al., 2013). U-shaped walls from glacier valleys provide a significant contribution to catchment erosion because their steepness favors rock fall and other gravity-driven sediment movements (Baartman et al., 2013). Glacier melt and associated processes such as landsliding (Emmer et al., 2016; Klimes et al., 2016) and glacial lake outburst floods (Vilimek, 2016) provide significant transport of large blocks into the fluvial domain. In the north, the Peruvian forearc has been intruded by various generations of magmatic intrusions (Haederle and Atherton, 2002) and their cooling has led to a dense network of fractures. Pre-fractured rock is easier to erode and may provide an additional source of larger boulders of granitic composition into the fluvial system. Granite is generally an abrasion-resistant type of rock and those clasts will retain their initial larger sizes longer while in transport. The southern

Earth Surf. Dynam. Discuss., doi:10.5194/esurf-2017-8, 2017
Manuscript under review for journal Earth Surf. Dynam.
Discussion started: 1 March 2017

(fore)arc region on the other hand, experiences active volcanism. Volcanic rock is generally softer and easier to break down and reduces the possibility of maintaining larger clasts in fluvial transport. This could provide an additional explanation for the generally larger grains in the north compared to the south.

4.5. Lithological and transport distance controls on sphericity

Studies have shown that lithologies and variation in the grain-size distribution of the supplied sediment play a role in controlling the fining rate within a stream through abrasion and fracturing (Attal and Lavé 2009; Litty and Schlunegger, 2017). Pebbles from different geological parent material expose variable predispositions for evolution during the fluvial processes. This appears to be corroborated by our observations. Rivers from the southern basins show more spherical gravels in correlation with the presence of volcanic rocks from the forearc region whereas the rivers from the northern basins show less spherical pebbles in correlation with the presence of intrusive rocks. The cooling of intrusive rocks in the northern Peruvian forearc has led to the formation of prefractured rocks. These rocks when eroded from the bedrock are more prolate and the supplied pebbles to the streams are then less spherical too. We then infer that the lithology of the parent material affects the shape of the pebbles.

We also consider a control of the transport distance on the N-S trends in the sphericity of the pebbles. As particles are transported over longer distances, abrasion tends to equalize the length of the three axes, thus making a particle more spherical. But this concept does not appear to be generally true. Indeed, pebbles flatten as effects of abrasion and 3D heterogeneities of bedrock that becomes more obvious with time and transport distance (Sneed and Folk, 1958). As the transport distances are larger for the southern basins than for the northern ones (Table 3), the pebbles should be less spherical in the southern basins than in the northern ones, which is what we can see in our data (Figure 3). We note that this is only valid if we assume a linear correlation between river length and transport time. The reincorporation of previously abraded gravels from earlier erosion and transport cycles that were temporarily stored in the catchment cannot be considered here.

5. CONCLUSIONS

Twenty-one rivers on the western Peruvian margin were analyzed to determine the relationships between fluvial processes, tectonics, climate and grain size and shape. The measurements of the grain sizes reveal a large spread from north to south for the *b*-axis with constant values of the D_{50} percentile and an increase of the D_{84} and D_{96} towards the north. The difference between the D_{50} and D_{96} percentiles is smaller in the south indicating that river sediments are better sorted in the south than in the north. In addition, the sphericity of the pebbles increases from south to north. A division in a northern and southern group of river basins was made. The southern group comprises the basins are located between 18.1°S and 15.6°S while the northern group comprises the catchments between 13.7°S and 7.3°S. These two groups show differences in their grain size distributions. Rivers in the southern group show better-sorted sediments and lower D_{84} and D_{96} values compared to basins of the northern group. Similarly, for gravel bars situated in the southern basins, correlations have been found between the D_{50} and the mean annual runoff. In the northern basins, the only correlation that has been found is a positive correlation between the gradient at sampling site and the D_{96}.

We primarily suggest an geomorphic control on the grain size pattern at the scale of the entire western Andean margin where larger basins host finer grained and better sorted material through a combination of selective entrainment and winnowing, the effects of which become more obvious with transport distance and thus larger basins. In addition, the overlaying north-south trend in the grain size could reflect a climatic control on the grain size distribution where a shift towards a more humid climate towards the north of Peru correlates with larger grains and worse sorted sediments. Superimposed to these controls, however, differences in hillslope-channel coupling relationships and complex patterns of sediment supply may perturb this large-scale pattern. Additionally, differences in the main lithologies along with different transport distance in-between the north and the south appear to have a control on the pebbles sphericity.

ACKNOWLEDGMENTS

This project is funded by the Swiss National Science Foundation (project Number 137516).

REFERENCES CITED

Abbühl, L.M., Norton, K.P., Jansen, J.D., Schlunegger, F., Aldahan, A., and Possnert, G., 2011, Erosion rates and mechanisms of knickzone retreat inferred from 10Be measured across strong climate gradients on the northern and central Andes Western Escarpment: Earth Surface Processes and Landforms, v. 36, p. 1464–1473.

Allen, G. H., Barnes, J. B., Pavelsky, T. M. and Kirby, E., 2013, Lithologic and tectonic controls on bedrock channel form at the northwest Himalayan front: Journal of Geophysical Research: Earth Surface, v. 118, no. 3, p. 1806-1825.

Attal, M. and Lavé, J., 2006, Changes of bedload characteristics along the Marsyandi River (central Nepal): Implications for understanding hillslope sediment supply, sediment load evolution along fluvial networks, and denudation in active orogenic belts: Geological Society of America Special Papers, v. 398, p.143-171.

Attal, M., Mudd, S. M., Hurst, M. D., Weinman, B., Yoo, K. and Naylor, M., 2015, Impact of change in erosion rate and landscape steepness on hillslope and fluvial sediments grain size in the Feather River basin (Sierra Nevada, California): Earth Surface Dynamics, v. 3, p. 201-222.

Atherton, M.P., 1984, The coastal batholith of Peru. In Andean Magmatis, p. 168-179, Birkhäuser Boston.

Autoridad Nacional de Agua, 2016. www.ana.gob.pe. Accessed 20th of November 2016.

Baartman, J. E., Masselink, R., Keesstra, S. D., & Temme, A. J., 2013. Linking landscape morphological complexity and sediment connectivity. Earth Surface Processes and Landforms, v. 38(12), p. 1457-1471.

Blissenbach, E., 1952. Relation of surface angle distribution to particle size distribution on alluvial fans: J. Sediment. Petrol., v. 22, p. 25–28.

Bookhagen, B. and Strecker, M. R., 2008, Orographic barriers, high-resolution TRMM rainfall, and relief variations along the eastern Andes, Geophysical Research Letters, v. 35, p. L06403.

Bull, W. B., 1991. Geomorphic responses to climatic change.

Bunte, K., Abt, S.R., 2001a. Sampling frame for improving pebble count accuracy in coarse gravel-bed streams. Journal of the American Water Resources Association, v. 37 (4), p. 1001- 1014.

Bunte, K., Abt, S.R., 2001b. Sampling surface and subsurface particle-size distributions in wadable gravel- and cobble-bed streams for analyses in sediment transport, hydraulics, and streambed monitoring. General Technical Report RMRS-GTR-74. United States Department of Agriculture; Forest Service; Rocky Mountain Research Station. Fort Collings, USA, p. 428.

Decou, A., von Eynatten H., Mamani M., Sempere T., and Wörner G., 2011, Cenozoic forearc basin sediments in Southern Peru (15–18°S): Stratigraphic and heavy mineral constraints for Eocene to Miocene evolution of the Central Andes, Sediment. Geol., v. 237(1), p. 55–72, doi:10.1016/j.sedgeo.2011.02.004.

DeVries, T. J., 1987, A review of geological evidence for ancient El Nino activity in Peru. J. Geophys. Res, v. 92, no. 14, p. 471–14.

Duller, R. A., Whittaker, A. C., Swinehart, J. B., Armitage, J. J., Sinclair, H. D., Bair, A. and Allen, P. A., 2012, Abrupt landscape change post-6 Ma on the central Great Plains, USA: Geology, v. 40, p. 871-874.

Earth Surf. Dynam. Discuss., doi:10.5194/esurf-2017-8, 2017
Manuscript under review for journal Earth Surf. Dynam.
Discussion started: 1 March 2017

Emmer, A., Vilímek, V., Huggel, C., Klimeš, J., & Schaub, Y., 2016. Limits and challenges to compiling and developing a database of glacial lake outburst floods. Landslides, p. 1-6.

Fedele, J. J. and Paola C., 2007, Similarity solutions for fluvial sediment fining by selective deposition: Journal of Geophysical Research: Earth Surface (2003–2012), v. 112.

Foreman, B. Z., Heller, P. L. and Clementz, M. T., 2012, Fluvial response to abrupt global warming at the Palaeocene/Eocene boundary: Nature, v. 491, no. 7422, p. 92-95

Foreman, B. Z., 2014, Climate-driven generation of a fluvial sheet sand body at the Paleocene–Eocene boundary in north-west Wyoming (USA): Basin Research, v. 26, no. 2, p. 225-241.

Garreaud, R. D., Vuille, M., Compagnucci, R., and Marengo, J., 2009, Present-day South American climate. Palaeogeography, Palaeoclimatology, Palaeoecology, v. 281, no. 3, p. 180-195.

Garreaud, R., and Aceituno, P., 2001, Interannual rainfall variability over the South American Altiplano. Journal of Climate, v. 14, no. 12, p. 2779-2789.

Gilboa, Y., 1977. The salinization in the alluvial aquifers of the coast of Peru, Bol. Soc. Geol. Peru, v. 57/58, p. 35 – 58.

Hack, J. T. , 1973. Stream-profile analysis and stream-gradient index. Journal of Research of the US Geological Survey, v. 1(4), p. 421-429.

Haederle, M., and Atherton, M.P., 2002, Shape and intrusion style of the Coastal Batholith, Peru. Tectonophysics, v. 345, no. 1, p. 17-28.

Heller, P. L. and Paola, C., 1992, The large-scale dynamics of grain-size variation in alluvial basins, 2: Application to syntectonic conglomerate: Basin Research, v. 4, no. 2, p. 91-102.

Hjulström, F., 1935, Studies in the morphological activity of rivers as illustrated by the river Fyris: Bulletin of the Geological Institution of the University of Uppsala, v 25, p. 221-528.

Hoey, T. B., 2010, Numerical simulation of downstream fining by selective transport in gravel bed rivers: Model development and illustration: Water Resources Research, v. 30, p. 2251-2260.

Hoey, T. B. and Ferguson, R., 1994, Numerical simulation of downstream fining by selective transport in gravel bed rivers: Model development and illustration: Water resources research, v.30, p. 2251-2260.

Howard, J.L., 1993. The statistics of counting clasts in rudites: a review with examples from the upper Paleogene of southern California, USA. Sedimentology 40, 157-174.

Huffman, G. J., Bolvin, D. T., Nelkin, E. J., Wolff, D. B., Adler, R. F., Gu, G. and Stocker, E. F., 2007, The TRMM multisatellite precipitation analysis (TMPA): Quasi-global, multiyear, combined-sensor precipitation estimates at fine scales. Journal of Hydrometeorology, v. 8, no. 1, p. 38-55.

Kodoma, Y., 1994, Downstream changes in the lithology and grain size of fluvial gravels, the Watarase River, Japan: Evidence of the role of abrasion in downstream fining: Journal of Sedimentary Research, Section A: Sedimentary Petrology and Processes, v. 64A, p. 68-75.

Koiter, A. J., Owens, P. N., Petticrew, E. L. and Lobb, D. A., 2013, The behaviour characteristics of sediment properties and their implications for sediment fingerprinting as an approach for identifying sediment source sin river basins: Earth Science Reviews, v. 125, p. 24-42.

Lisle, T.E., Iseya, F. and Ikeda, H., 1993, Response of a channel with alternate bars to a decrease in supply of mixed-size bed load: A flume experiment: Water resources research, v. 29, p. 3623–3629.

Litty and Schlunegger, 2017. Controls on Pebbles’ Size and Shape in Streams of the Swiss Alps. The Journal of Geology., v. 125, p. 101–112.

Litty, C., Lanari, P., Burn, M., and Schlunegger, F., 2017, Climate-controlled shifts in sediment provenance inferred from detrital zircon ages, Western Peruvian Andes. Geology. v. 45; no. 1; p. 59–62.

Londoño, A. C., 2008. Pattern and rate of erosion inferred from Inca agricultural terraces in arid southern Peru. Geomorphology, v. 99(1), p. 13-25.

Macharé, J., Sébrier, M., Huaman, D., & Mercier, J. L., 1986. Tectónica cenozoica de la margen continental peruana. Boletín de la Sociedad geológica del Perú, v. 76, p. 45-77.

Maddy, D., 1997, Uplift-driven valley incision and river terrace formation in southern England, Journal of Quaternary Science, v. 12, p. 539–545.

Earth Surf. Dynam. Discuss., doi:10.5194/esurf-2017-8, 2017
Manuscript under review for journal Earth Surf. Dynam.
Discussion started: 1 March 2017

Earth Surface Dynamics
Discussions
Open Access
EGU

Marcus, W.A., Ladd, S.C., Stoughton, J.A., Stock, J.W., 1995. Pebble counts and the role of user-dependent bias in documenting sediment size distributions. Water Resources Research, v. 31 (10), p. 2625-2631.

Margirier, A., Audin, L., Carcaillet, J., Schwartz, S., and Benavente, C., 2015, Tectonic and climatic controls on the Chuquibamba landslide (western Andes, southern Peru). Earth Surface Dynamics, 3(2), 281-289.

McLaren, P. and Bowles, D., 1985, The Effects of Sediment Transport on Grain-Size Distributions: Journal of Sedimentary Petrology, v. 55, p. 457-470.

Molnar, P., Anderson, R. S., Kier, G., and Rose, J., 2006, Relationships among probability distributions of stream discharges in floods, climate, bed load transport, and river incision. Journal of Geophysical Research: Earth Surface, v. 111(F2).

Morgan, R.P. and Rickson, R. J., 2003. Slope stabilization and erosion control: a bioengineering approach. Taylor & Francis.

Mukasa, S.B., 1986, Zircon U-Pb ages of super-units in the Coastal batholith, Peru: Implications for magmatic and tectonic processes: Geological Society of America Bulletin, v. 97, p. 241–254.

NASA, 2000, SRTM 90 m Digital Elevation Data from the CGIAR-CSI Consortium for Spatial Information, University of Maryland, College Park, Maryland.

Paola, C., Heller, P. L. and Angevinet, C. L., 1992a, The large-scale dynamics of grain-size variation in alluvial basins, 1: Theory: Basin Research, v. 4, p. 73-90.

Paola, C., Parker, G., Seal, R., Sinha, S. K., Southard, J. B. and Wilcock, P. R., 1992b, Downstream fining by selective deposition in a laboratory flume: Science, v. 258, p. 1757-1757.

Paola, C. and Seal, R., 1995, Grain size patchiness as a cause of selective deposition and downstream fining: Water Resources Research, v. 31, p. 1395-1407.

Parker, G., 1991, Selective sorting and abrasion of river gravel. 1: Theory: Journal of Hydraulic Engineering, v. 117, no. 2, p. 131-147.

Rabatel, A., Francou, B., Soruco, A., Gomez, J., Cáceres, B., Ceballos, J. L., ... & Scheel, M., 2013. Current state of glaciers in the tropical Andes: a multi-century perspective on glacier evolution and climate change. Cryosphere, v. 7(1), p. 81-102.

Earth Surf. Dynam. Discuss., doi:10.5194/esurf-2017-8, 2017
Manuscript under review for journal Earth Surf. Dynam.
Discussion started: 1 March 2017

Ramos, V. A., 2010. The tectonic regime along the Andes: Present-day and Mesozoic regimes. Geological Journal, v. 45(1), p. 2-25.

Rasband, W.S., ImageJ, U. S. National Institutes of Health, Bethesda, Maryland, USA, http://imagej.nih.gov/ij/, 1997-2016.

Rice, S. and Church, M., 1998, Grain size along two gravel-bed rivers: Statistical variation, spatial pattern and sedimentary links: Earth Surface Processes and Landforms, v. 23, p. 345-363.

Robinson, R. A. and Slingerland, R. L., 1998, Origin of fluvial grain-size trends in a foreland basin: the Pocono Formation on the central Appalachian basin: Journal of Sedimentary Research, v. 68, no. 3.

Saillard, M., Hall, S.R., Audin, L., Farber, D.L., Regard, V., and Hérail, G., 2011. Andean coastal uplift and active tectonics in southern Peru: 10 Be surface exposure dating of differentially uplifted marine terrace sequences (San Juan de Marcona,~ 15.4 S). Geomorphology, v. 128(3), p. 178-190.

Schildgen, T. F., Hodges, K. V., Whipple, K. X., Reiners, P. W. and Pringle, M. S., 2007, Uplift of the western margin of the Andean plateau revealed from canyon incision history, southern Peru. Geology 35, 523–526.

Schildgen, T. F., Hodges, K. V., Whipple, K. X., Pringle, M. S.,. van Soest, M, and Cornell, K., 2009, Late Cenozoic structural and tectonic development of the western margin of the central Andean Plateau in southwest Peru, Tectonics, v. 28, TC4007, doi:10.1029/2008TC002403.

Schumm, S. A. and Stevens, M. A., 1973, Abrasion in place: a mechanism for rounding and size reduction of coarse sediments in rivers: Geology, v. 1, p. 37-40.

Shields, A., 1936, Anwendung der Ahnlichkeitsmekanik und der Turbulenzforschung auf die Geschiebebewegung, Mittelung der preussischen Versuchsanstalt für Wasserbau und Schiffbau, 26. (Berlin).

Sneed, E.D., and Folk, R.L., 1958. Pebbles in the lower Colorado River, Texas a study in particle morphogenesis. The Journal of Geology, 114-150.

Steffen, D., Schlunegger, F., and Preusser, F., 2010, Late Pleistocene fans and terraces in the Majes valley, southern Peru, and their relation to climatic variations. International Journal of Earth Sciences, v. 99(8), p. 1975-1989.

Earth Surf. Dynam. Discuss., doi:10.5194/esurf-2017-8, 2017
Manuscript under review for journal Earth Surf. Dynam.
Discussion started: 1 March 2017

Sternberg, H., 1875, Untersuchungen über längen-und Querprofil geschiebeführender Flüsse, Z. Bauwes., 25, 486–506.

Surian, N., 2002, Downstream variation in grain size along an Alpine river: analysis of controls and processes: Geomorphology, v. 43, p. 137-149.

Trauerstein, M., Norton, K. P., Preusser, F., and Schlunegger, F., 2013, Climatic imprint on landscape morphology in the western escarpment of the Andes. Geomorphology, v. 194, p. 76-83.

Vidal, J. C., 1993, Geologia de los cuadrangulos de Huambo y Orcopampa, v 46. Instituto Geologico Minero y Metalurgico, Lima.

Viveen, W., Schoorl, J. M., Veldkamp, A., Van Balen, R. T., Desprat, S., & Vidal-Romani, J. R., 2013. Reconstructing the interacting effects of base level, climate, and tectonic uplift in the lower Miño River terrace record: a gradient modelling evaluation. Geomorphology, v. 186, p. 96-118.

Wells, L. E., 1990, Holocene history of the El Niño phenomenon as recorded in flood sediments of northern coastal Peru. Geology, v. 18, no. 11, p. 1134-1137.

Whittaker, A. C., Cowie, P. A., Attal, M., Tucker, G. E. and Roberts, G. P., 2007, Bedrock channel adjustment to tectonic forcing: Implications for predicting river incision rates: Geology, v. 35, no. 2, p.103-106.

Whittaker, A. C., Attal, M. and Allen, P.A., 2010, Characterising the origin, nature and fate of sediment exported from catchment perturbed by active tectonics. Basin Research. v. 22. p. 809-828.

FIGURE CAPTIONS

Table 1: Location of the sampling sites with the altitude in meters above sea level. The table also displays grain size results together with the rivers' and basins' properties and hydrological properties.

Earth Surf. Dynam. Discuss., doi:10.5194/esurf-2017-8, 2017
Manuscript under review for journal Earth Surf. Dynam.
Discussion started: 1 March 2017

Table 2: Location of the sampling sites in the Majes basin and grain size results in the Majes basin.

Table 3: Differences of the basins characteristics between the southern group of basins and the northern group as showed in Figure 1 and 4A.

Figure 1: A: Map of the studied basins showing the sampling sites and the western escarpment (western escarpment modified after Trauerstein et al., 2013). The southern and northern group of basins represent catchments displaying differences in terms of their sizes and relationships with grain sizes (see Results) **B:** Geological map of the western Peruvian Andes. **C:** Map of the precipitation rates showing the spatial extend of the ITCZ, modified after Huffman et al., 2007.

Figure 2: Geological map of the Majes basin overlain by the precipitation pattern (Precipitation data from Steffen et al., 2010., where the black dashed lines show precipitation rates (mm/yr). GS1 to GS5 represent sites where grain size data has been collected. The right corner shows the Majes river long profile.

Figure 3: A: Grain size results for the intermediate (*b*)-axis of the pebbles in the streams from north to south at the sampling sites presented in Figure 1. **B:** Ratio between the intermediate axis and the long (*a*)-axis from north to south at the sampling sites presented in Figure 1.

Figure 4: Grain size results along the Majes River.

Earth Surf. Dynam. Discuss., doi:10.5194/esurf-2017-8, 2017
Manuscript under review for journal Earth Surf. Dynam.
Discussion started: 1 March 2017

Figure 5: Grain size data. **A:** D_{50} versus distance from the uppermost edge of the western Escarpment (taken from Trauerstein et al., 2013). **B:** D_{96} versus distance from the uppermost edge of the western Escarpment. **C:** D_{50} versus gradient averaged over a 500 m-long reach. **D:** D_{96} versus gradient averaged over a 500 m-long reach. **E:** D_{50} versus mean annual runoff. **F:** D_{96} versus maixum annual runoff. We only present the plot of the river properties versus the D_{50} and D_{96}. We found the same absence of correlation for the 84th percentile.

Figure 6: **A:** D_{50} versus the mean annual runoff normalized over the catchment area for the southern basins. **B**: D_{96} versus local gradient at the sampling site for the northern basins.

Earth Surf. Dynam. Discuss., doi:10.5194/esurf-2017-8, 2017
Manuscript under review for journal Earth Surf. Dynam.
Discussion started: 1 March 2017

Earth Surface Dynamics
Discussions
Open Access

Sample name/ name of the river	Altitude (m)	Latitude (°)	Longitude (°)	D50 (cm)	D84 (cm)	D96 (cm)	b/a	Catchment area (km2)	Gradient at the sampling site	Distance form the western escarpment (km)
Tacna	231	-18.12	-70.33	2.3	6.2	10.0	0.70	899	0.015	48
Rio Sama Grande	455	-17.82	-70.51	2.5	5.5	10.6	0.67	2150	0.013	73
Ilo / Rio Osmore	1072	-17.29	-70.99	2.6	5.1	7.8	0.70	1783	0.018	53
Rio Tambo	145	-17.03	-71.69	1.5	3.6	7.5	0.69	12885	0.051	141
Tambillo / Rio Sihuas	117	-16.34	-72.13	2.0	6.0	10.0	0.69	1708	0.019	70
Camana / Rio Majes	69	-16.51	-72.64	5.2	8.7	11.6	0.67	17401	0.005	188
Ocona / Rio Ocona	14	-16.42	-73.12	4.8	6.8	10.0	0.71	16084	0.004	192
Nasca / Rio Grande	15	-15.85	-74.26	1.3	3.0	6.0	0.71	1412	0.014	48
Chacaltana / Rio Ica	3	-15.63	-74.64	2.9	6.4	9.6	0.73	4677	0.003	88
Humay District / Rio Pisco	400	-13.73	-75.89	3	6.6	13		3649	0.013	62
Chinca Alta / Rio San Juan	75	-13.47	-76.14	1.3	3.8	7.6	0.69	3090	0.01	78
Rio Canete	23	-13.12	-76.39	2	4.6	8.8	0.72	6029	0.01	100
Rio Omas	33	-12.67	-76.65	1.6	4.8	8.8	0.73	2322	0.0076	78
Rio Lurin	40	-12.25	-76.89	3	5	8.8	0.74	1572	0.022	70
Lima / Rio Chillon	402	-11.79	-76.99	5.3	10.5	15.5		1755	0.018	51
Rio Chancay	72	-11.61	-77.24	5.5	8.3	12.5	0.74	3059	0.01	66
Rio Supe	74	-11.07	-77.59	2.8	7.7	13		4306	0.012	82
Rio Pativilca	10	-10.72	-77.77	1.8	3.6	6		4607	0.014	74
Huarmey	24	-10.07	-78.16	1.7	3.4	5.2		2072	0.004	78
Rio Santa	80	-8.97	-78.62	2	5.4	9	0.72	12313	0.005	65
San Martin de Porres	67	-7.32	-79.48	2.9	6.3	10		3882	0.007	126

Table 1 : Location of the sampling sites with the altitude in meters above sea level.
The table also displays grain size results together with the rivers' and basins' properties and hydrological properties

Earth Surf. Dynam. Discuss., doi:10.5194/esurf-2017-8, 2017
Manuscript under review for journal Earth Surf. Dynam.
Discussion started: 1 March 2017

Sample name/ name of the river	Hydrology Gauging station name	Latitude (°)	Longitude (°)	Altitude (m)	Mean annual runoff (m3/s)	Maximum annual runoff (m3/s)	years of record	Number of measured months	Catchment area (m2)	Mean runoff (m3/s) / catchemnt area (m2)	Maximum runoff (m3/s) / catchemnt area (m2)
Tacna	Ticapampampa	-17.983	-70.133	1400	2.13	3.99	1950-1984 1986-1989	438	8.99.E+08	2.37E-09	4.44E-09
Rio Sama Grande	Coruca	-17.616	-70.45	852	2.34	3.57	2005-2009	43	2.15.E+09	1.09E-09	1.66E-09
Ilo / Rio Osmore	Bocatoma Torata - Río Torata	-17.13	-70.9	1614	1.23	1.67	2005-2016	139	1.78.E+09	6.90E-10	9.37E-10
Rio Tambo	Puente Santa Rosa	-17.69	-71.69	160	27.94	46.93	2011-2016	23	1.29.E+10	2.17E-09	3.64E-09
Tambillo / Rio Sihuas	Lluclla	-16.18	-72.0333	1900	2.21	2.91	1977-1981	38	1.71.E+09	1.29E-09	1.70E-09
Camana / Rio Majes	Puente Carretera Camana	-16.6	-72.73	122	73.31	185.26	1960-1986	122	1.74.E+10	4.21E-09	1.06E-08
Ocona / Rio Ocona	Puente Ocana	-16.421	-73.115	23	95.46	170.57	1984, 86, 2004-2005, 2007, 08, 14	64	1.61.E+10	5.94E-09	1.06E-08
Nasca / Rio Grande	La Pena	-14.53	-75.166	500	4.1	9.33	1950-1990	84	1.41.E+09	2.90E-09	6.61E-09
Chacaltana / Rio Ica	Huamani	-13.83	-75.58	800	10.68	36.65	1922-1947	291	4.68.E+09	2.28E-09	7.84E-09
Humay District / Rio Pisco	Letrayoc	-13.65	-75.716	720	26.54	38.03	2014-2016	26	3.65.E+09	7.27E-09	1.04E-08
Chinca Alta / Rio San Juan	Conta	-13.45	-75.983	350	14.43	36.14	2011-2016	57	3.09.E+09	4.67E-09	1.17E-08
Rio Canete	Toma Imperial	-13	-76.216	400	52.66	113.95	1950-1971	236	6.03.E+09	8.73E-09	1.89E-08
Rio Omas	La Capilla	-12.52	-76.49	424	15.64	48.00	1938-2016	419	2.32.E+09	6.74E-09	2.07E-08
Rio Lurin	Manchay Bajo	-12.17	-76.85	206	4.72	12.26	1950-1984	196	1.57.E+09	3.00E-09	7.80E-09
Lima / Rio Chillon	Puente Huarabi	-11.66	-76.86	800	8.56	30.12	1919-1947	315	1.76.E+09	4.88E-09	1.72E-08
Rio Chancay	Santo Domingo	-11.38	-77.05	697	14.5	37.53	2014-2016	699	3.06.E+09	4.74E-09	1.23E-08
Rio Supe	El Liman	-10.83	-77.58	107	2.99	6.26	1964-1972	34	4.31.E+09	6.94E-10	1.45E-09
Rio Pativilca	Alpas	-10.61	-77.5	400	47.80	90.65	1950-1975	298	4.61.E+09	1.04E-08	1.97E-08
Huarmey	Puente Huamba	-9.96	-77.86	550	5.8	14.12	1973-1984	67	2.07.E+09	2.80E-09	6.82E-09
Rio Santa	Condorcerro	-8.65	-78.25	450	136	289	1977-2016	466	1.23.E+10	1.10E-08	2.35E-08
San Martin de Porres	Yonan	-7.25	-79.1	428	28.6	59.3	1975-2016	210	3.88.E+09	7.37E-09	1.53E-08

Table 1 : Location of the sampling sites with the altitude in meters above sea level.
The table also displays grain size results together with the rivers' and basins' properties and hydrological properties

Earth Surf. Dynam. Discuss., doi:10.5194/esurf-2017-8, 2017
Manuscript under review for journal Earth Surf. Dynam.
Discussion started: 1 March 2017

	Distance from the coast (km)	Altitude (m)	Latitude (°)	Longitude (°)	D50	D84	D96	b/a
GS1	20	69	-16.51	-72.64	5.2	8.7	11.6	0.67
GS2	45	283	-16.37	-72.49	4.8	10	15	0.69
GS3	57	378	-16.28	-72.45	5.4	12.7	21	0.65
GS4	90	700	-16.00	-72.48	3.3	12	22.5	0.67
GS5	106	882	-15.86	-72.45	6.2	19	31	0.71

Table 2: Location of the sampling sites in the Majes basin and grain size results in the Majes basin.

Earth Surf. Dynam. Discuss., doi:10.5194/esurf-2017-8, 2017
Manuscript under review for journal Earth Surf. Dynam.
Discussion started: 1 March 2017

	Southern basins	Northern basins
Mean D84	5.7	5.8
Mean D96	9.2	9.85
Sorting	Well sorted	Badly sorted
Mean catchment area (km2)	7200	4000
Mean gradient at sampling site	0.016	0.009
Mean distance from escarpment (km)	100	69

Table 3: Differences of the basins characteristics between the southern group of basins and the northern group as showed in Figure 1 and 4A.

Earth Surf. Dynam. Discuss., doi:10.5194/esurf-2017-8, 2017
Manuscript under review for journal Earth Surf. Dynam.
Discussion started: 1 March 2017

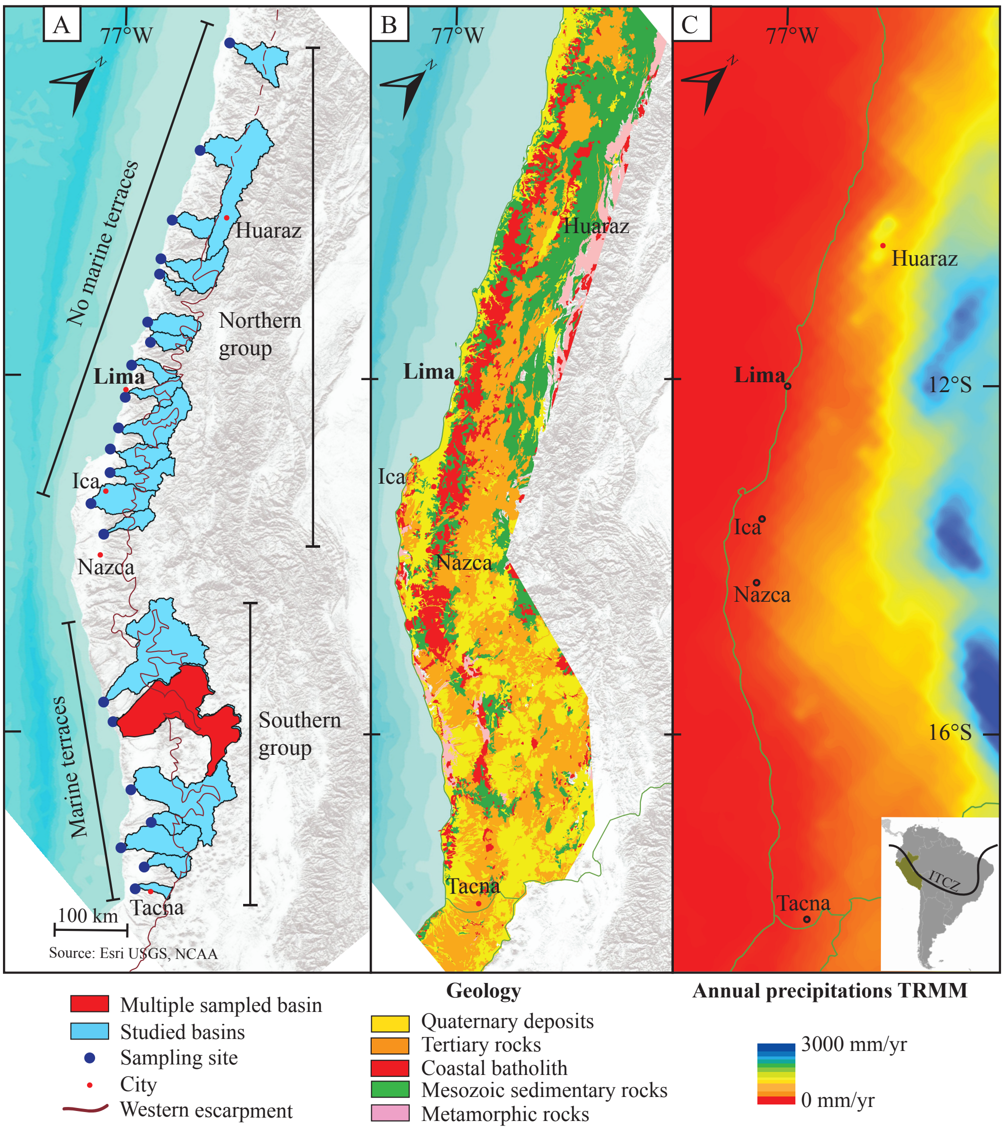

Figure 1: A: Map of the studied basins showing the sampling sites and the western escarpment (western escarpment modified after Trauerstein et al., 2013). The southern and northern group of basins represent catchments displaying differences in terms of their sizes and relationships with grain sizes (see Results) **B:** Geological map of the western Peruvian Andes. **C:** Map of the precipitation rates showing the spatial extend of the ITCZ, (modified after Huffman et al., 2007.)

Earth Surf. Dynam. Discuss., doi:10.5194/esurf-2017-8, 2017
Manuscript under review for journal Earth Surf. Dynam.
Discussion started: 1 March 2017

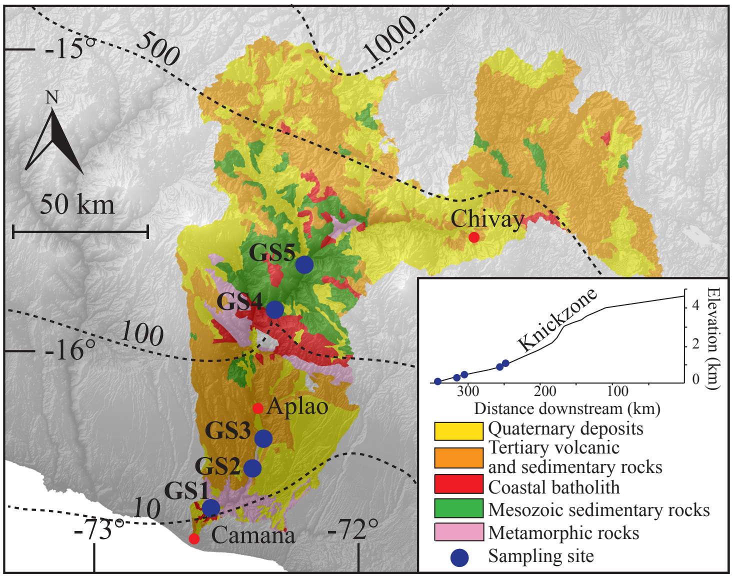

Figure 2: Geological map of the Majes basin overlain by the precipitation pattern (Precipitation data from Steffen et al., 2010., where the black dashed lines show precipitation rates (mm/yr). GS1 to GS5 represent sites where grain size data has been collected. The right corner shows the Majes river long profile.

Earth Surf. Dynam. Discuss., doi:10.5194/esurf-2017-8, 2017
Manuscript under review for journal Earth Surf. Dynam.
Discussion started: 1 March 2017

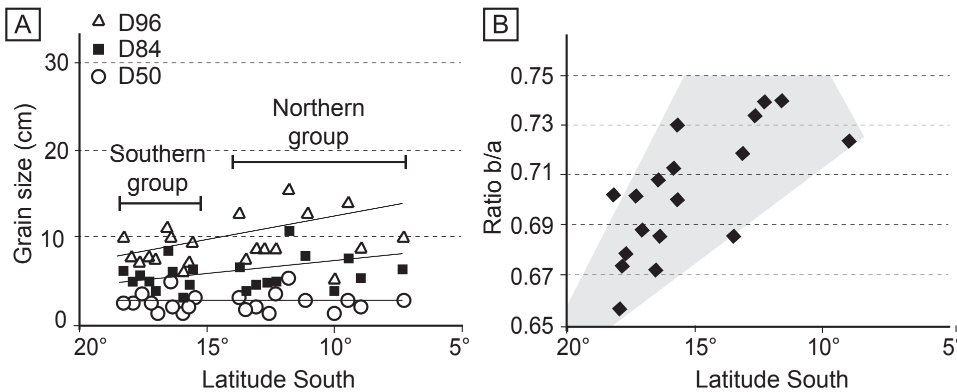

Figure 3: A: Grain size results for the intermediate (b)-axis of the pebbles in the streams from north to south at the sampling sites presented in Figure 1. **B:** Ratio between the intermediate axis and the long (a)-axis from north to south at the sampling sites presented in Figure 1.

Earth Surf. Dynam. Discuss., doi:10.5194/esurf-2017-8, 2017
Manuscript under review for journal Earth Surf. Dynam.
Discussion started: 1 March 2017

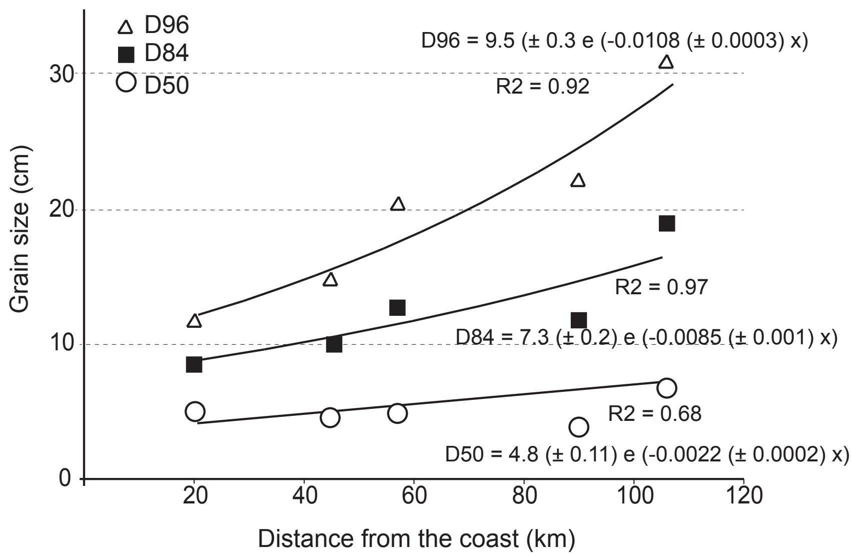

Figure 4: Grain size results along the Majes River.

Earth Surf. Dynam. Discuss., doi:10.5194/esurf-2017-8, 2017
Manuscript under review for journal Earth Surf. Dynam.
Discussion started: 1 March 2017

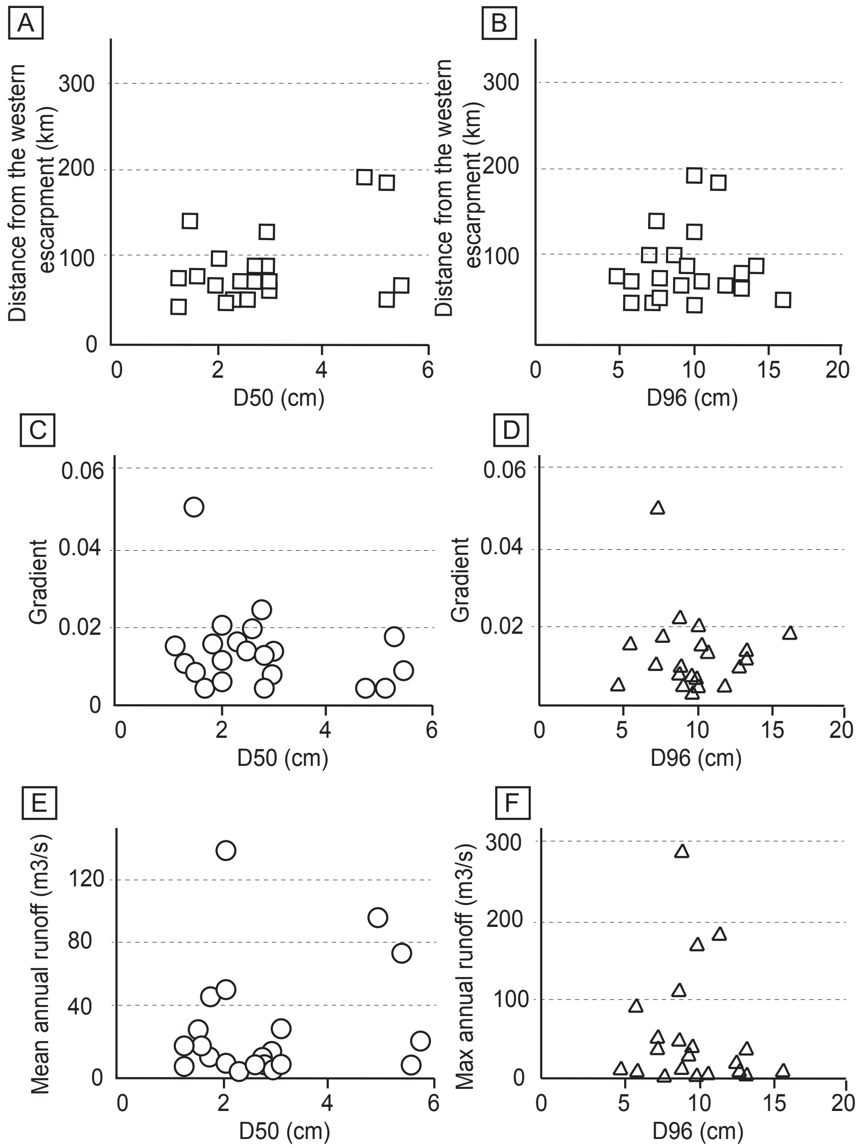

Figure 5: Grain size data. ***A:*** D50 versus distance from the uppermost edge of the western Escarpment (taken from Trauerstein et al., 2013). **B:** D96 versus distance from the uppermost edge of the western Escarpment. **C:** D50 versus gradient averaged over a 500 m-long reach. **D:** D96 versus gradient averaged over a 500 m-long reach. **E:** D50 versus mean annual runoff. **F:** D96 versus maixum annual runoff. We only present the plot of the river properties versus the D50 and D96. We found the same absence of correlation for the 84th percentile.

Earth Surf. Dynam. Discuss., doi:10.5194/esurf-2017-8, 2017
Manuscript under review for journal Earth Surf. Dynam.
Discussion started: 1 March 2017

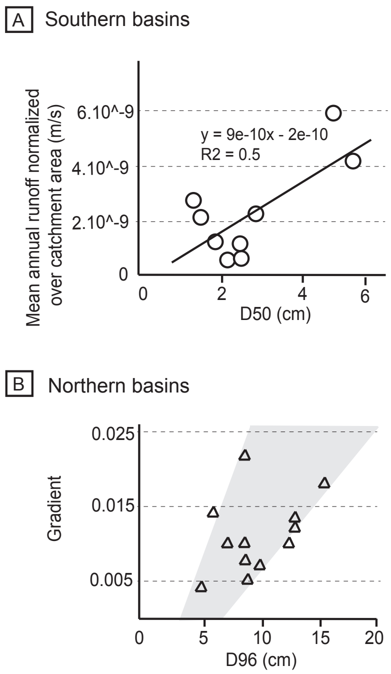

Figure 6: A: D50 versus the mean annual runoff normalized over the catchment area for the southern basins. **B:** D96 versus local gradient at the sampling site for the northern basins.